N6-methyladenosine (m6A)-mediated messenger RNA signatures and the tumor immune microenvironment can predict the prognosis of hepatocellular carcinoma

Shen Shen[1,2#], Jingya Yan[1,2#], Yize Zhang[1,2], Zihui Dong[1,2], Jiyuan Xing[1,2], Yuting He[1]

[1]Gene Hospital of Henan Province, Precision Medicine Center, The First Affiliated Hospital of Zhengzhou University, Zhengzhou, China; [2]Department of Infectious Diseases, the First Affiliated Hospital of Zhengzhou University, Zhengzhou, China

Contributions: (I) Conception and design: All authors; (II) Administrative support: Y He, S Shen; (III) Provision of study materials or patients: J Yan, Z Dong; (IV) Collection and assembly of data: Y Zhang; (V) Data analysis and interpretation: S Shen, J Xing; (VI) Manuscript writing: All authors; (VII) Final approval of manuscript: All authors.

[#]These authors contributed equally to this work.

Correspondence to: Yuting He. Gene Hospital of Henan Province, Precision Medicine Center, The First Affiliated Hospital of Zhengzhou University, No.1 Jianshe Road, Zhengzhou 450052, China. Email: fccheyt1@zzu.edu.cn.

Background: N6-methyladenosine (m6A)-mediated ribonucleic acid (RNA) methylation is considered to be the most significant and abundant epigenetic modification in eukaryotic cells, and plays an essential role in the carcinogenesis and molecular pathogenesis of hepatocellular carcinoma (HCC). However, the relationship between m6A regulation and immune cell infiltration of the tumor immune microenvironment (TIME) has not yet been clarified. We aimed to investigate the roles of m6A RNA gene regulators in HCC immune regulation and prognosis.

Methods: The Cancer Genome Atlas (TCGA) database was used, and unsupervised clustering of 21 m6A regulators was performed based on differential gene expression. Gene Set Variation Analysis (GSVA), single-sample Gene Set Enrichment Analysis (ssGSEA), the empirical Bayes method, and m6A scores were used in our analyses.

Results: Of 433 samples, 101 (23.22%) had m6A regulatory factor mutations. From these, we identified three m6A subtypes, which correlated with different TIME phenotypes: immune rejection, immune infiltration, and immune deficiency. Tumors with low methyltransferase-like 3 (*METTL3*) expression had increased infiltration of dendritic cells (DCs) in the TIME. Reduced *METTL3* expression also led to an overall increase in expression of major histocompatibility complex (MHC) molecules, costimulatory molecules, and adhesion molecules. The m6A subtypes were scored and analyzed for correlations. Patients with epithelial-mesenchymal transition (EMT) subtypes had lower m6A scores than the other three molecular subtypes. Survival analysis found that patients with low m6A scores had better overall survival [hazard ratio (HR) 1.6 (1.1–2.3)] and a 1.16 times better 5-year survival rate than patients with high m6A scores (56% *vs.* 48%).

Conclusions: Our results demonstrated that three different m6A modification subtypes contribute to immune regulation in HCC and have potential as novel prognostic indicators and immune therapeutic targets.

Keywords: N6-methyladenosine (m6A); Hepatocellular carcinoma (HCC); tumor immune microenvironment (TIME); methyltransferase-like 3 (*METTL3*); survival

Submitted Oct 19, 2020. Accepted for publication Dec 08, 2020.
doi: 10.21037/atm-20-7396
View this article at: http://dx.doi.org/10.21037/atm-20-7396

Introduction

Hepatocellular carcinoma (HCC) remains a high incidence malignancy with high mortality rate and poor prognosis worldwide. It has been reported that there are approximately 850,000 new HCC patients annually, with about 500,000 deaths due to HCC-associated diseases (1,2). Hepatitis B and C viral infections, excess alcohol consumption, aflatoxin B1 exposure, obesity, diabetes, and metabolic diseases are major risk factors for the development of HCC (3). Owing to the difficulty in making an early diagnosis, HCC patients are typically diagnosed at an advanced stage of the disease, and thus, treatments are generally associated with a low survival rate, high risk of recurrence, malignant metastasis, as well as a high risk of selection and spreading of drug resistance (4). Recently, immune therapies, such as immune checkpoint inhibition, have been used in advanced HCC to modify the carcinogenic process and to augment adaptive immunity (5). It has been shown that the tumor immune microenvironment (TIME), which is composed of both pro- and anti-tumor immune cells, can be reprogrammed by tumor-derived factors, which are involved in immune evasion and tumor progression (6,7). Accumulating evidence supports a role for the TIME in determining HCC progression, recurrence, metastasis, and poor outcome (8,9). Tumor-infiltrating immune cells (TIICs) are important components of the TIME and have been shown to be significant predictors of HCC survival (10). However, correlations between TIME parameters and HCC genesis and development are still poorly understood (10).

Currently, the most well studied messenger ribonucleic acid (mRNA) modification is N6-methyladenosine (m6A). It is the most pervasive internal mRNA modification (10), and correlates with tumor progression (11). Previous studies have shown that m6A demethylation of the fat mass and obesity-associated protein (FTO) is up-regulated and promotes tumor proliferation and metastasis in breast cancer (12,13). However, the role of the m6A modification in HCC tumorigenesis remains unclear.

We hypothesized that m6A may regulate HCC tumorigenesis and progression by regulating the immune system and thus may be a therapeutic drug target for HCC. To evaluate this hypothesis, data from The Cancer Genome Atlas (TCGA) were used as an effective cohort, and data from the Gene Expression Omnibus (GEO) database were used as a validation cohort. Genes associated with the immune microenvironment were downloaded from the Immunology Analysis Portal database (https//www.immport.org/shared/genelists), analyzed, and immune phenotypes were classified by immune scores. We validated the different m6A modification patterns and explored the relationship between immune infiltration and m6A regulation. We also identified three different immune phenotypes: the immune rejection phenotype, the immune inflammation phenotype, and the immune desert phenotype, and found that formation of the tumor microenvironment plays a role in the phenotype. We combined m6A modification patterns and immune infiltration phenotypes to establish a system to estimate HCC prognosis.

We present the following article in accordance with the REMARK reporting checklist (available at http://dx.doi.org/10.21037/atm-20-7396).

Methods

Data collection

The work-flow of this study is illustrated in Figure S1A. All related information was downloaded from TCGA data portal (http://cancergenome.nih.gov/). And the study was conducted in accordance with the Declaration of Helsinki (as revised in 2013). Data cohorts with missing information were removed. Data collection, refinement, and model statistics are summarized in Table S1. RNA sequence data from the National Cancer Institute's (NCIs) Genomic Data Commons (GDC, https://gdc.cancer.gov/about-data/publications/pancanatlas), Fragments Per Kilobase per total Million mapped reads (FPKM), and TCGA biolinks were also used (14,15). Data were analyzed using the statistical software package R, version 3.6.1. Raw data were processed into R/Bioconductor.

Unsupervised gene cluster analysis

We used clustering, a resampling-based clustering algorithm, to analyze the m6A gene profiles of HCCs. A total of 21 m6A regulators, including eight writers, two erasers, and 11 readers were analyzed. We performed unsupervised cluster analysis with a consistent clustering algorithm and the Consensus Cluster Plus package as described previously (16).

Gene Set Variation Analysis (GSVA) and functional annotation

For an in-depth analysis of the biological processes that

associate with the different m6A modification patterns, the "GSVA" R package for GSVA enrichment analysis was utilized. The gene set "c2.cp.kegg. v6.2. symbols" was downloaded from the MSigDB database and used to run GSVA analysis. For functional annotation of genes, we utilized cluster analysis and a false discovery rate <0.05.

Estimation of the immune cells infiltrating the TIME

A gene set of a variety of human immune cell subtypes was obtained from Charoentong *et al.* (17). Single-sample Gene Set Enrichment Analysis (ssGSEA) calculates separate enrichment scores for each sample and gene pair. This analysis showed the relative abundance of each cell type that infiltrated the TIME for each sample.

Classification of m6A phenotypes based on differential gene expression

To validate and classify m6A-associated genes, differentially expressed gene (DEG) analysis (fold-changes) and statistical computations of the two conditions were conducted using the EBSeq R package (https://bioconductor.org/packages/release/bioc/html/EBSeq.html).

Construction of m6A gene markers and m6A scoring

To validate m6A regulator modifications in HCC samples, we established a scoring system to estimate *m6A* gene characteristics. To establish *m6A* gene markers, DEGs of the different m6A clusters were normalized to extract overlapping genes, the unsupervised clustering method was used to analyze the overlapping data, and patients were divided into multiple groups for in-depth analysis. The number and stability of gene clusters were defined by the consistent clustering algorithm. We then used a univariate Cox regression model to analyze the association of each gene cluster with prognosis. We selected principal component 1 and principal component 2 as signature scores. Subsequently, we defined the m6a score using a method like that used in analyzing gene-gene interactions (GGIs): $m6A\ Score = \Sigma\ (PC1i + PC2i)$.

Analysis of m6A modifications and their immune-related signatures in HCC

To investigate associations between m6A modifications and the immune microenvironment, we downloaded immune-related genes from the ImmPort database (http://www.immport.org), and identified prognostic gene signatures based on genes with independent prognostic values as determined previously (18). Our m6A scoring system revealed that m6A gene characteristics are associated with particular biological pathways.

Statistical analysis

DEGs were applied in this study with the threshold of absolute log2-fold-change >1 and an adjusted P value <0.05 using the R package "limma". The overall survival rate was evaluated using the log-rank test with Kaplan-Meier estimation. Differences between the groups were evaluated by analysis of variance (ANOVA). All P values were two-sided, and P values <0.05 were considered significant. Comparative studies were analyzed using the Kruskal-Wallis test and Wilcoxon test. *P<0.05, **P<0.01, ***P<0.001. All statistics were calculated using R language.

Results

Expression of m6A regulators in HCC

To better understand the search strategy and selection of datasets for comprehensively understand m6A regulation in HCC progression, we constituted a flow chart of this study (Figure S1A). In total, 371 patients were involved in this study and three clusters were identified. The transcription levels of 21 m6A regulators, which included 11 readers, eight writers, and two erasers, as well as the copy number variations (CNVs) and somatic mutations of these regulators, were described in a previous study (19). The chromosomal locations of the amplification mutations were distributed randomly and unequally across the chromosomes (*Figure 1A*). Of 64 HCC samples, 44 contained mutations related to m6A modifications (68.75% mutation rate). The most prevalent mutation were found in the *KIAA1429* (8%) and *LRPPRC* (8%) genes, followed by *HNRNPC* (6%) and *YTHDC2* (6%) (*Figure 1B*). The 21 m6A regulators exhibited widespread gene gain and loss mutations, *KIAA1429* and *YTHDF3* contained the most gain mutation type, while *ALKBH5* and *ZC3H13* had the most frequent loss mutation type (*Figure 1C*). We also explored the 21 regulators in tumor tissue compared with normal tissue, and easily identified the two subgroups; the red spot represented normal tissue and the blue spot represented tumor tissue (*Figure 1D*).

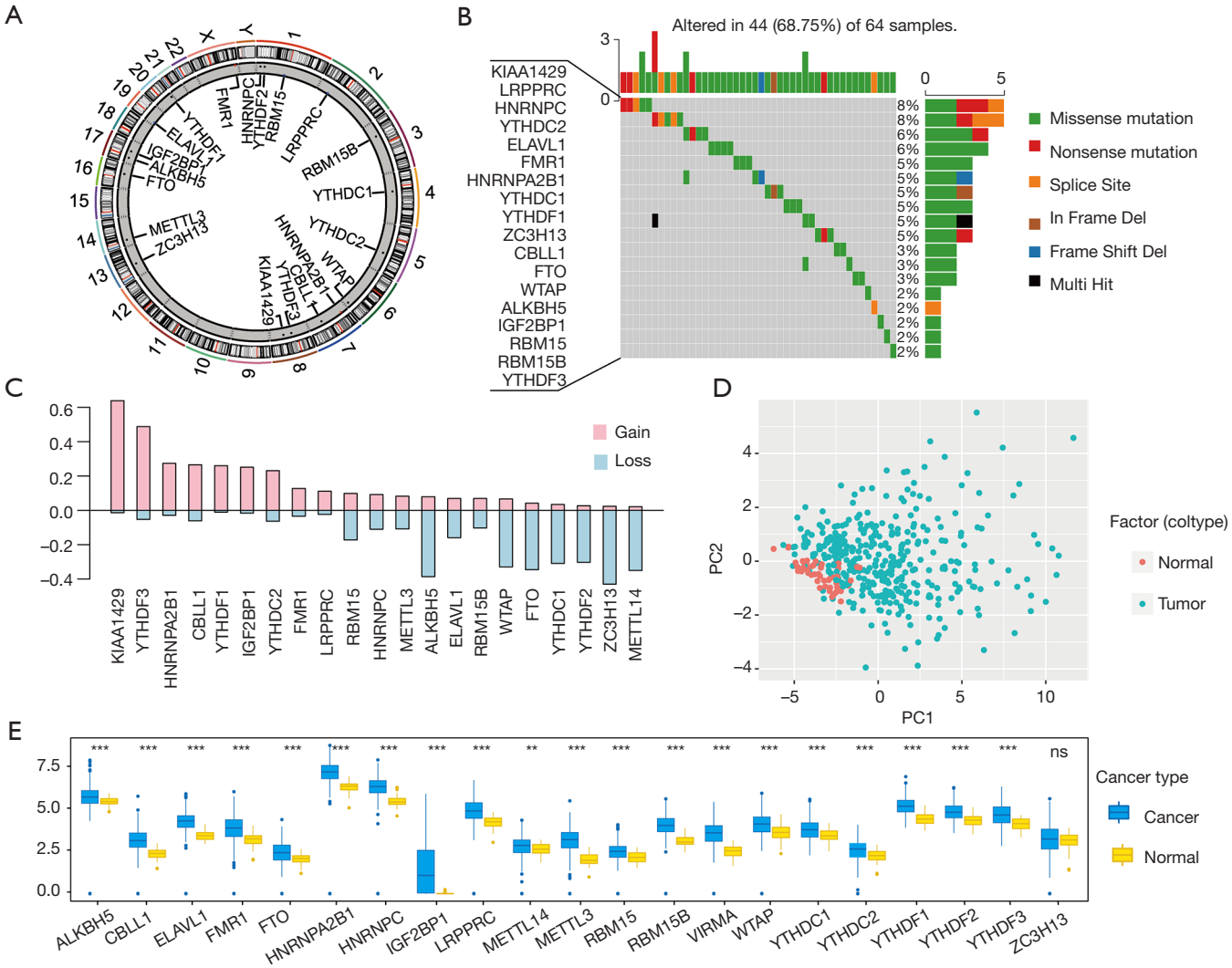

Figure 1 Overview of m6A gene locus and gene information. (A) The m6A regulators mutation location. (B) Waterfall plot of m6A regulators mutation gene and mutation type. (C) Frequency plots of copy number gains (in green) and losses (in red) defined in all m6A regulators. (D) Regulators could be divided into two subgroups (red and green) based on the gene expression level. (E) Comparison of gene expression level of 21 regulators between the normal and tumor tissue cohort. **P<0.01, ***P<0.001. m6A, N6-methyladenosine.

To further investigate the overall survival between the regulators, HCC patients were divided into mutated subgroup and wide type subgroup based on whether they were combined with m6A mutation information. Obviously, the mutated subgroups had a poor prognosis in *YTHDF1* [P=0.018, hazard ratio (HR) =4.7], *LRPPRC* (P=0.003, HR =6.44), and *FTO* (P=4.12e7, HR =11.3) (Figure S1B). We also performed a meta-analysis, and the results revealed that the regulators have prognostic potential in HCC cohorts (Figure S1C). The mean expression levels of m6A regulators in HCC specimens and normal tissues are shown in *Figure 1E*; the difference was significant and m6A regulators were highly expressed in both tumor tissue and normal tissue. In this study, we mapped the gene somatic mutation information of 21 m6A regulators between tumor tissue and normal tissue, and confirmed that m6A modification plays an important role in HCC tumorigenesis and progression.

m6A regulators have close relationship with cellular crucial functional pathways regulation

In order to comprehensively explain the crosslink among

the 21 m6A regulators, we divided 21 m6A regulators into three clusters as illustrated in *Figure 2A*. Through GSVA of functional genes, we determined the biological roles of the m6A regulators. The expression of genetic information of the m6A regulators was controlled through intricate regulatory networks and a complex regulatory relationship. The overall survival curve implied a significant survival advantage for cluster 2 (*P<0.0001, *Figure 2B*).

In the present study, we explored the relationship between different modification patterns and biological functional activities. The results indicated that three clusters exhibit significant pathway enrichment. The cluster 1-associated pathways gather on translation functions, such as olfactory transduction, neuroactive ligand receptor interaction, arachidonic acid metabolism complements and coagulation cascades, folate biosynthesis, arginine and proline metabolism, metabolism of xenobiotics by cytochrome, glutathione metabolism and Parkinson's disease cardiac muscle contraction, amyotrophic lateral sclerosis, prion diseases, and autoimmune diseases. Cluster 2 functional pathways were significantly enriched in the ERBB signaling pathway, cell cycle signaling pathway, cell adhesion, as well as other pathways related to cell matrix adhesion and carcinogenesis, such as colorectal cancer, chronic myeloid leukemia, adherent's junction, the ERBB signaling pathway, endometrial cancer, the cell cycle, oocyte meiosis, RNA degeneration, ubiquitin mediated proteolysis, basal transcription factors, non-homologous end joining, and thyroid cancer (*Figure 2C*). The third cluster-associated functional pathways act in metabolism pathways (*Figure 2D*). Our results implied that m6A regulators participated in many important cellular activities, including cellular metabolism regulation, nuclear factor regulation, signal transitional regulation, and carcinogenesis.

m6A regulators have a close relationship with the infiltration of immune cells

Next, we estimated the enrichment score of immune cells among the three clusters and identified the differences in the infiltration of immune cells among clusters 1–3. The box plot exhibited significant differences in most immune cells, including activated B cells, activated cluster of differentiation (CD)4+T cells, activated CD8+T cells, $^{\gamma\delta}$T cells, regulatory T cells, type 1 helper cells, type 17 helper cells, activated dendritic cells (DCs), CD56 bright natural killer (NK) cells, CD56 dim NK cells, eosinophils, macrophages, and mast cells (*Figure 3A*).

To further investigate the biological behaviors among the three m6A modification clusters, pathway enrichment analysis was applied. Our results indicated that the transforming growth factor beta (TGF-β) pathway, angiogenesis, and the tumor EMT process were remarkably different among the clusters (*Figure 3B*). Our research suggested that the three types of regulators were involved in crucial functional regulations with different pathways. According to the GSVA analysis, the 21 m6A regulators were classified as either an immune rejected phenotype, an immune inflamed phenotype, or an immune desert phenotype based on the infiltration of immune cells (*Figure 3A,B*).

We then focused on methyltransferase like 3 (*METTL3*), and the immune score of different *METTL3* expression subgroups showed a weak difference (*Figure 3C*). Furthermore, Spearman correlation analysis was performed for TIME infiltration and the m6A regulators (*Figure 3D*). *METTL3* expression correlated with many of the TIME infiltrating immune cells and the immune score. Our study implied that the infiltration of CD4+ T cells, type 1 T helper cells, type 2 T helpers, CD56 bright NK cells, eosinophils, macrophages, mast cells, monocytes, and neutrophils exhibited a significant difference between high and low *METTL3* expression (Figure S2A), indicating that low *METTL3* expression resulted in increased TIME-associated immune cell infiltration.

Subsequently, we estimated the gene expression of immune checkpoint molecules and receptors, and discovered that CD80, CD86, intercellular adhesion molecule (ICAM) 1, ICAM3, and programmed cell death ligand 1 (PDL1) gene expression showed differences across different *METTL3* expression levels (Figure S2B). We then evaluated the enrichment score of some crucial cell activity pathways between two clusters, and the box plot exhibited significant differences in the TGF-β pathway, T cell activation, angiogenesis, and the tumor EMT process (Figure S2C). These results indicated that the m6A regulators play key roles in immune cell infiltration and characteristic TIME formation.

The transcriptome and clinical features of m6A regulators

To further identify the cellular biological behavior and in-depth mechanisms of the m6A regulators, we performed unsupervised cluster analysis on m6A phenotype-related genes to divide patients into one of four different clusters based on the m6A modified genomic phenotypes

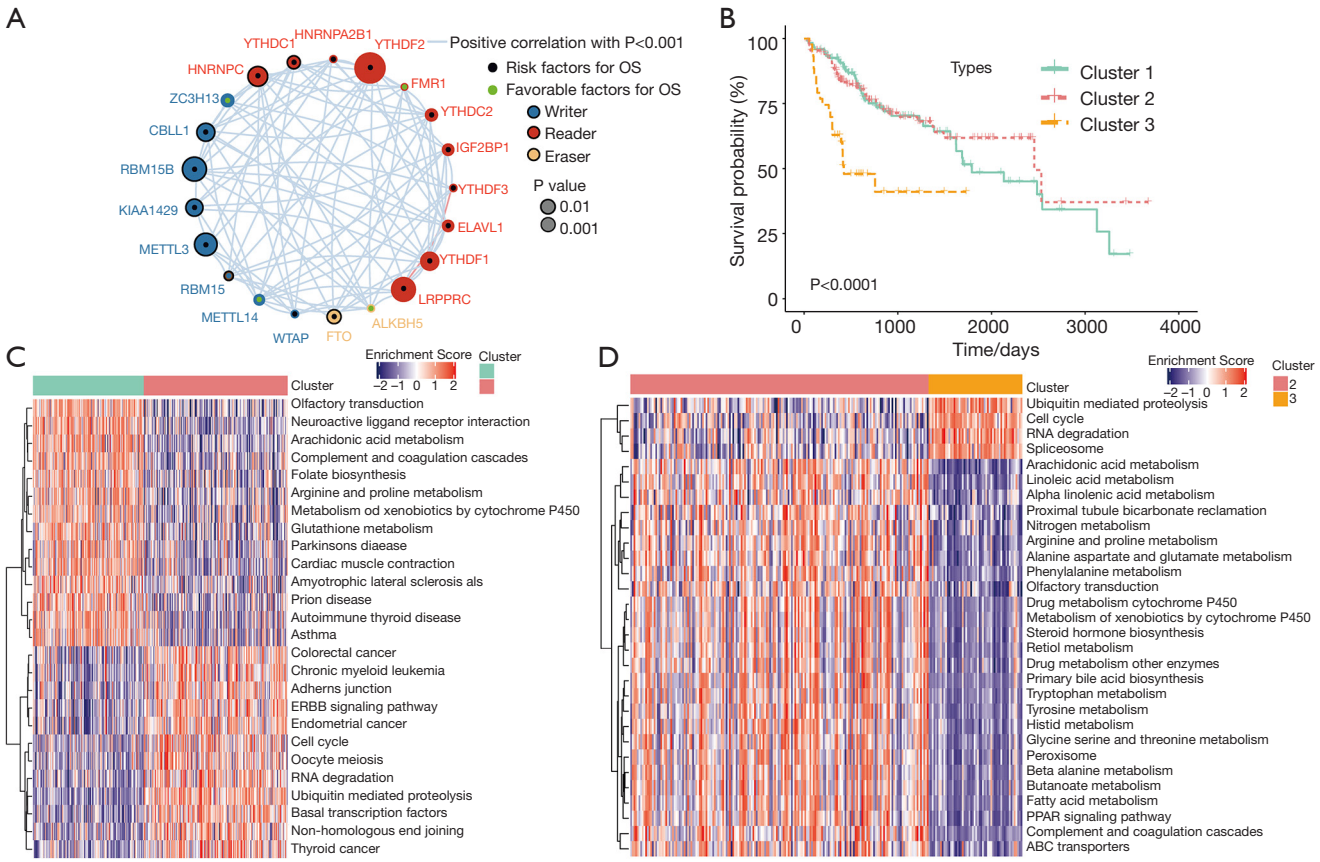

Figure 2 Crosslinks between 21 m6A regulators and associated biological activities. (A) Landscape and inner crosslink between 21 m6A regulators. (B) Kaplan-Meier curve of survival probability between three clusters. (C) Cluster enrichment analysis of biological activities between cluster 1 and cluster 2. (D) Cluster enrichment analysis of biological activities between cluster 2 and cluster 3. m6A, N6-methyladenosine.

(*Figure 4A*). Based on the m6A regulator classifications, we confirmed that cluster 1, with the abundant immune cell infiltration subgroup, exhibited a better prognosis and survival probability (*Figure 4B*). Among the three immune cell infiltration-associated subgroups, expression of regulatory factors of 21 regulators differed significantly (*Figure 4C*).

Further analysis of the matrix-related pathways revealed that the gene expression level of the m6A regulators suggested significantly different expression levels of immune related functional annotation and activation of matrix pathways, including CD8+T cells effector, angiogenesis, the cell cycle, cell cycle regulator, deoxyribonucleic acid (DNA) damage repair, DNA replication, EMT1, Fanconi anemia, homologous recombination, mismatch repair, nucleotide excision repair, and Pan-F-TBRS (*Figure 4D*). Here, we confirmed that the 21 regulators were classified into three gene clusters based on gene expression and cluster analysis. The box plots illustrated that the 21 regulators gene expression clusters were consistent with the functional classification.

The m6A regulators gene expression classification with immune infiltration

To better annotate the functions of m6A-related genes with immune cells, our analysis results implied that the infiltration of activated CD4+ T cells, regulatory T cells, type 17 T helper cells, CD56 bright NK cells, CD56 dim NK cells, and eosinophils exhibited significant differences between the three clusters (*Figure 5A*). To explore the roles of m6A-related phenotypes in the modulation of the TIME, we analyzed the expression of chemokines and cytokines in the three m6A gene clusters. Interferon gamma (*IFN-γ*), *CD8A*, T-Box transcription factor 2 (*TBX2*), and tumor necrosis factor (*TNF*) showed significant differences

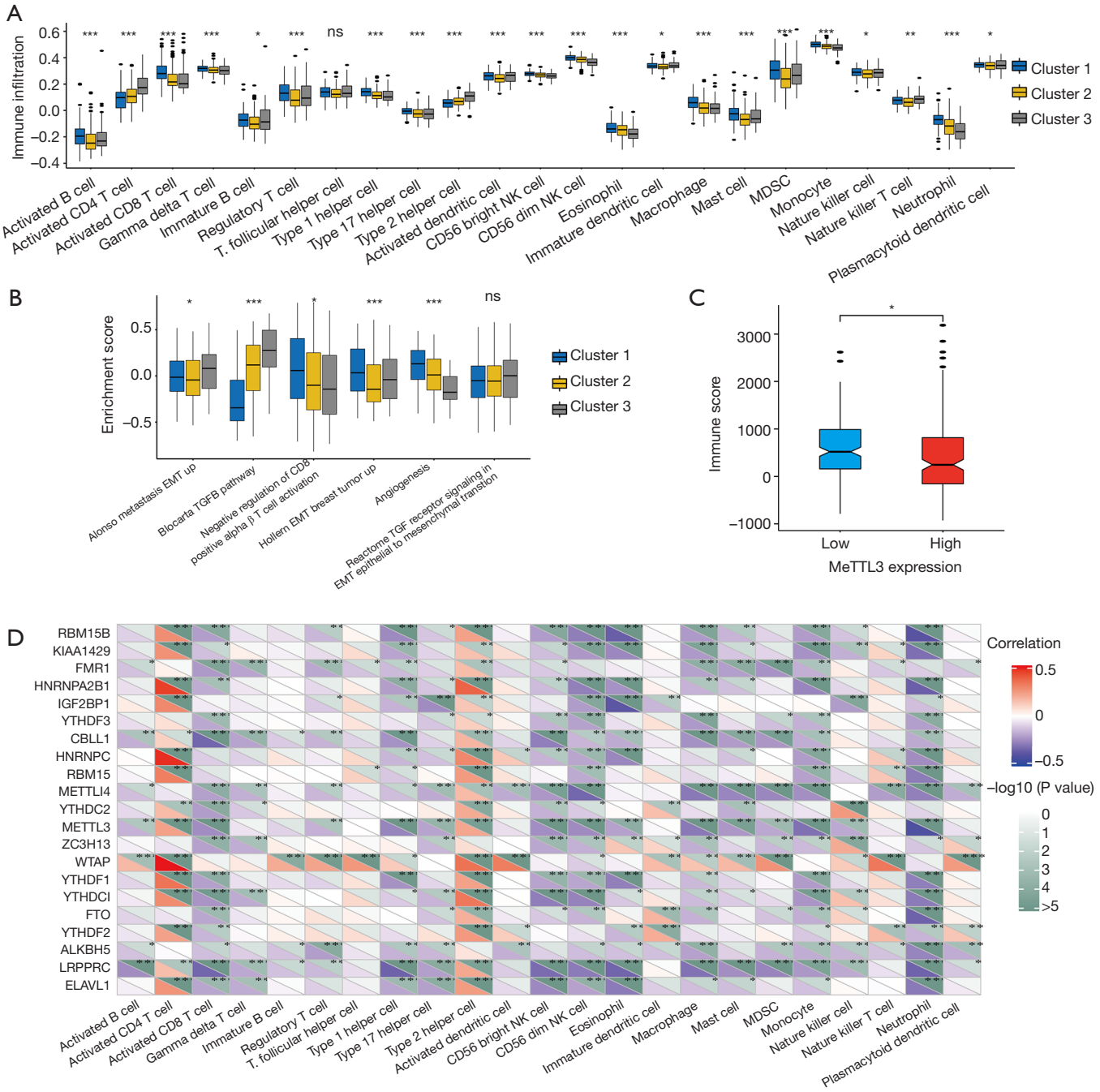

Figure 3 Immune cell infiltration and immune associated classification among m6A regulators. (A) Comparison between different immune cells infiltration in three clusters. (B) Comparison of cellular biological activities with enriched regulation pathways among three clusters. (C) Comparison of the immune score between the high and low *METTL3* expression subgroups. The immune score exhibited a weak difference between high and low *METTL3* expression levels. (D) Correlation between m6A regulators and biological pathways in the HCC cohort. The Spearman analysis was applied in this study. Negative correlation was marked with blue and positive correlation with orange. *P<0.05, **P<0.01, ***P<0.001. m6A, N6-methyladenosine.

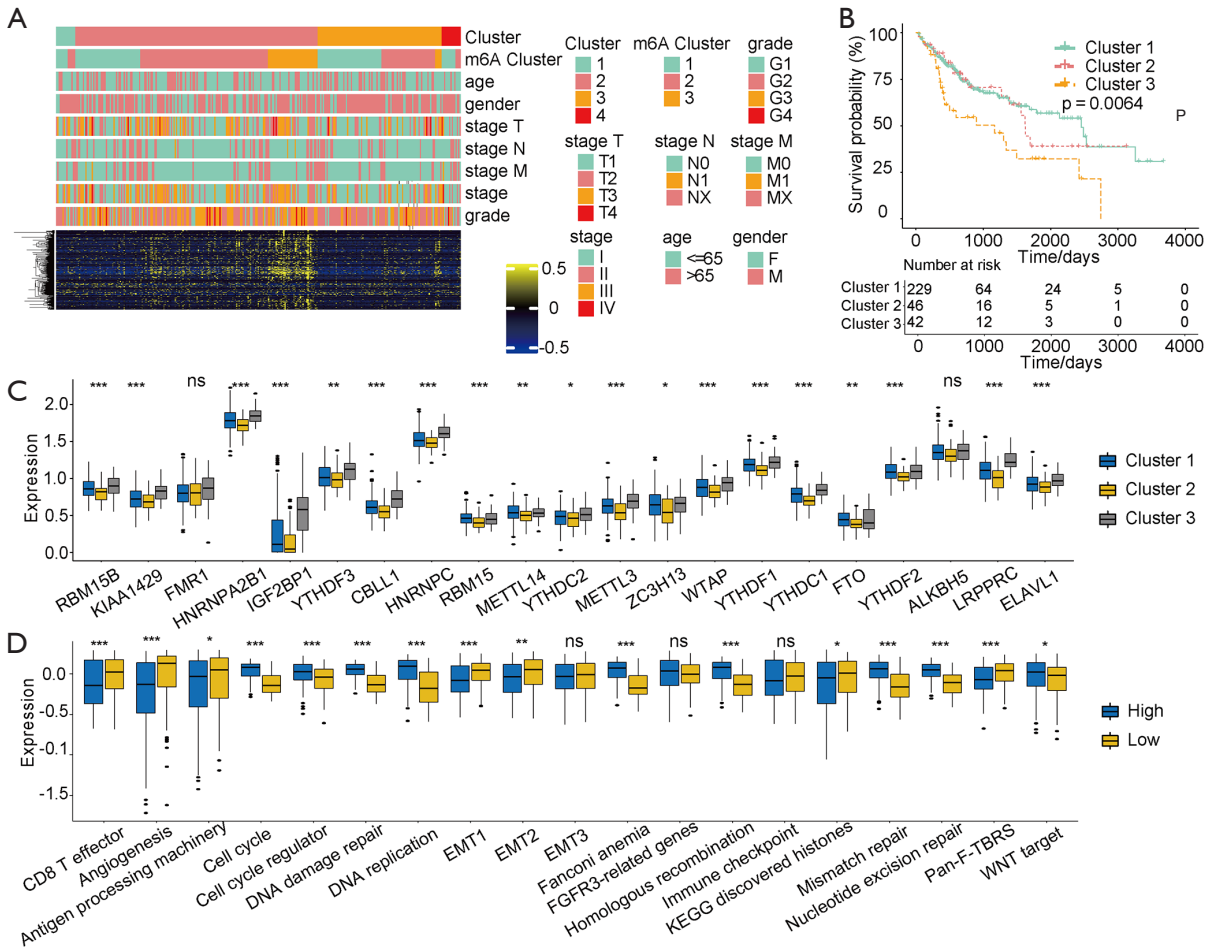

Figure 4 Clinical information in different m6A regulators. (A) m6A regulators were divided into four clusters based on gene expression. Related clinical information was involved in this cluster enrichment analysis. (B) Comparison of overall survival rate between the three different subgroups. (C) Comparison of m6A regulators gene expression levels among the three clusters. (D) Comparison of high and low immune score clusters in cellular activities and biological related pathways. m6A, N6-methyladenosine. *P<0.05, **P<0.01, ***P<0.001.

among the three clusters. Other cytokines exhibited no or weak differences between these clusters (*Figure 5B*). In *Figure 5C,D*, we estimated the gene expression of immune checkpoint molecules and receptors and found that *HAVCR2*, *CD80*, *PDCD1*, *TIGIT*, *CD86*, *COL4A1*, *ZEB*, *TGFB2*, and *TWIST1* gene expression showed remarkable differences between the three clusters, which suggested that these immune checkpoints had a significant relationship with the m6A regulator classification.

We further investigated the prognostic value of the m6A scores for HCC. HCC patients were divided into high and low m6A score groups, and the survival of these groups was compared. The overall survival for the low score m6A group was better than the high score group [P=0.019, HR 1.6 (1.1–2.3)]. The 5-year survival rate was 56% for the high m6A score group and 48% for the low score group (*Figure 5E*). The area under the curve (AUC) in patients treated with immunotherapy was 0.768 (*Figure 5F*). Our data demonstrated that the m6A evaluation scores based on modification patterns were correlated with immune or matrix activation, which affects tumor immune infiltrates and patient prognosis.

Discussion

Globally, HCC is still a lethal malignancy with a poor prognosis. The tumorigenesis mechanism of HCC must be elucidated to improve prognosis, identify biomarkers,

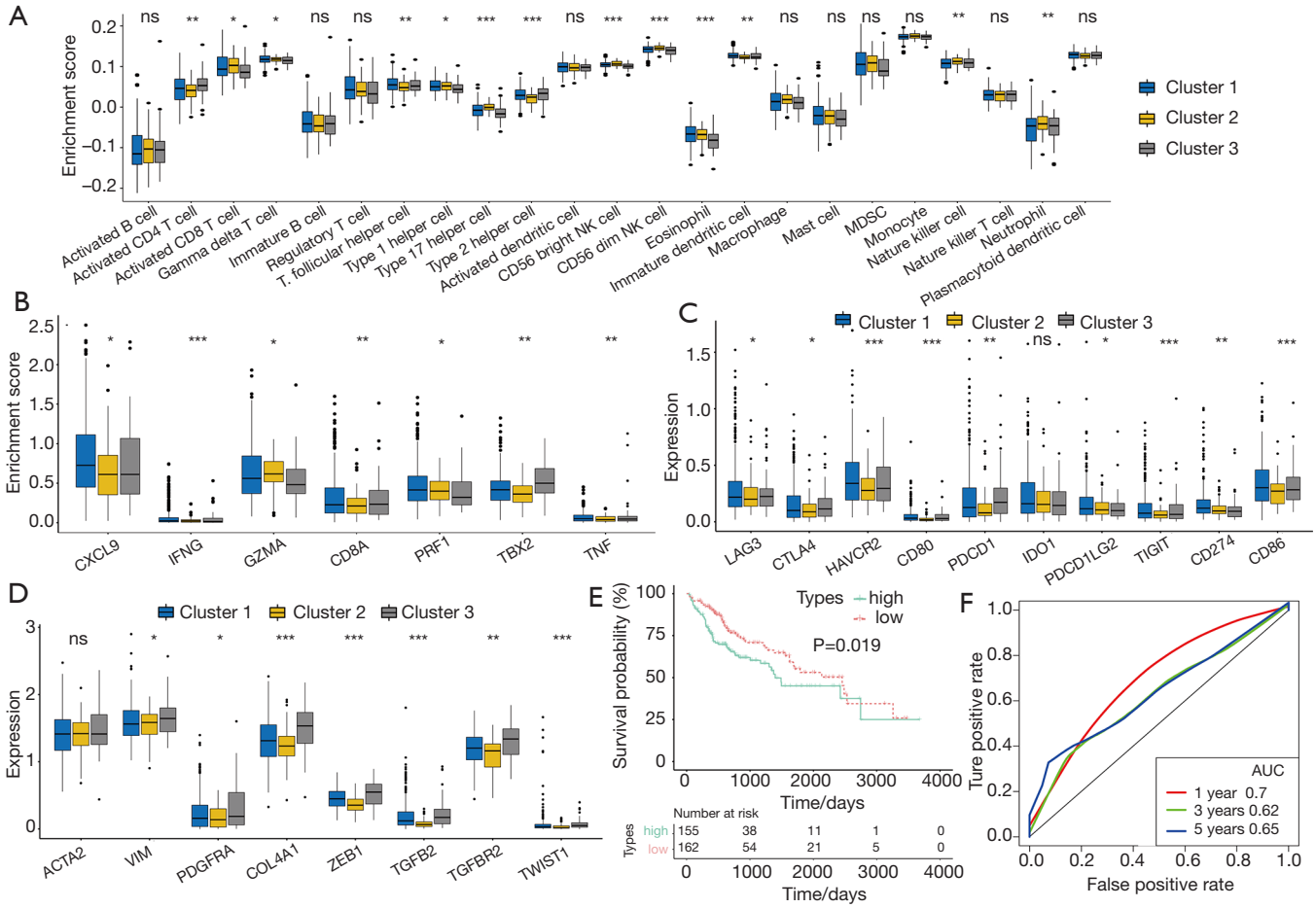

Figure 5 Comparison of different kinds of immune infiltration and prognosis analysis. (A) Comparison of enrichment score with different immune cells infiltration in the three clusters. (B) Comparison of enrichment score with different immune-related cytokines expression among the three clusters. (C) Expression level comparison of different immune checkpoint targets and associated receptors in the three clusters. (D) Expression comparison of m6A regulator-related kinases in the three clusters. (E) Overall survival analysis between the high and low immune score subgroups. (F) AUC of m6A regulators' signature validation of the survival value of the risk score. m6A, N6-methyladenosine. *P<0.05, **P<0.01, ***P<0.001.

and develop effective therapeutic strategies. The liver is the largest immune-related organ, and the immune system plays a definitive role in oncogenesis (20,21). Recent studies have indicated that aberrant mRNA modifications contribute to HCC prognosis and overall survival. Currently, m6A is the most well studied post-transcriptional mRNA modification, and evidence suggests that this modification epigenetically affects mRNA processing, translation, and stability (22). Dysregulation of the m6A modification has been shown to be associated with the initiation and progression of various cancers. Thus, exploring the relationship between m6A regulation and the TIME could lead to the design of immune-based targeted therapies for HCC.

METTL3 is a crucial oncogene in several cancers and has been shown to be up-regulated in gastric cancer (23), prostate carcinoma (24), and osteosarcoma (25). Also, methyltransferase like 14 (*METTL14*) has been shown to play a crucial role in the RNA epigenetics of colorectal cancer, and thus, has prognostic value (26). It is also been shown that *YTHDF2* suppresses cancer cell migration via m6A-associated modification (26). In the present study, we identified three different m6A modification patterns and their relationship with the infiltration of immune cells, such as NK cells, macrophages, eosinophils, mast cells, myeloid-derived suppressor cells (MDSCs), and plasma cell-like DCs, into the HCC microenvironment. Based on

the infiltration of immune cells and the immune score, we identified three different immune-associated phenotypes of the HCC tumor environment: immune excluded, immune inflamed, and immune desert. The immune excluded phenotype is characterized by the presence of T cells at the periphery of cancer nests. In the immune excluded phenotype of bladder cancer, there was no PD-L1 expression and only a few tumor-infiltrating lymphocytes (TILs) were present (27). Mariathasan *et al.* found that combination therapy with TGF-blocking and anti-PD-L1 antibodies decreased TGF signaling in stromal cells, facilitated concentration of T cells in the centers of tumors, and provoked vigorous anti-tumor immunity and tumor regression (28). Zhao *et al.* demonstrated that the immune inflamed phenotype of triple-negative breast cancers is characterized by the infiltration of CD8+ T cells into the tumor parenchyma, indicating that these patients are more likely to benefit from immune checkpoint inhibitor therapy (29). Job *et al.* reported that the inflamed subtype is characterized by massive T lymphocyte infiltration as well as activation and upregulation of inflammatory and immune checkpoint pathways. This phenotype is associated with a prolonged survival prognosis (30). Thus, patients with the immune inflamed phenotype may benefit from immunotherapy. In this study, we found that the immune desert phenotype is characterized by CD8 cell deficiency and is associated with a poor prognosis.

The TIME can predict patient survival in most cancer types, and m6A modification has been shown to affect cell infiltration in the TIME and the epigenetic regulation of the immune response in gastric cancer. M6A has also been shown to regulate the innate immune response by targeting type I interferons (18,31). In the innate immune system, neoantigen-specific immunity is regulated by mRNA methylation via the m6A-binding protein *YTHDF1* (32). In this study, we explored m6A regulatory factor-mediated TIME cell infiltration and found more DCs, including activated DCs, immature DCs, and plasma cell-like DCs in tumors with low *METTL3* expression, indicating that *METTL3*-mediated m6A methylation modification activates DCs in the TIME, thereby enhancing the anti-tumor immune response.

Conclusions

Our findings demonstrated that numerous immune-related genes regulated by m6A modification contribute to the immune phenotype. Moreover, we validated a novel model of m6A modification and immune-related gene regulation to predict HCC prognosis. The immune score and immune classification systems may lead to novel therapeutic targets for HCC.

Acknowledgments

We thank the patients and investigators who participated in TCGA and the GEO for providing the data analyzed in this study.

Funding: This study was supported by funds from the National Natural Science Foundation of China (No 81902832); the Science and Technology Research Project of Henan Province (No 192102310117 and 202102310115); and the Gandan Xiangzhao Research Fund (No GDXZ2019001 and GDXZ2019007).

Footnote

Reporting Checklist: The authors have completed the REMARK reporting checklist. Available at http://dx.doi.org/10.21037/atm-20-7396

Conflicts of Interest: All authors have completed the ICMJE uniform disclosure form (available at http://dx.doi.org/10.21037/atm-20-7396). The authors have no conflicts of interest to declare.

Ethical Statement: The authors are accountable for all aspects of the work in ensuring that questions related to the accuracy or integrity of any part of the work are appropriately investigated and resolved. The study was conducted in accordance with the Declaration of Helsinki (as revised in 2013).

References

1. Kempinska K, Malik B, Borkin D, et al. Pharmacologic

Inhibition of the Menin-MLL Interaction Leads to Transcriptional Repression of PEG10 and Blocks Hepatocellular Carcinoma. Mol Cancer Ther 2018;17:26-38.
2. Llovet JM, Zucman-Rossi J, Pikarsky E, et al. Hepatocellular carcinoma. Nat Rev Dis Primers 2016;2:16018.
3. Yang JD, Hainaut P, Gores GJ, et al. A global view of hepatocellular carcinoma: trends, risk, prevention and management. Nat Rev Gastroenterol Hepatol 2019;16:589-604.
4. Xie QL, Liu Y, Zhu Y. Chromosome region maintenance 1 expression and its association with clinical pathological features in primary carcinoma of the liver. Exp Ther Med 2016;12:59-68.
5. Ou Q, Yu Y, Li A, et al. Association of survival and genomic mutation signature with immunotherapy in patients with hepatocellular carcinoma. Ann Transl Med. 2020;8:230.
6. Gajewski TF, Schreiber H, Fu YX. Innate and adaptive immune cells in the tumor microenvironment. Nat Immunol 2013;14:1014-22.
7. Azambuja JH, Ludwig N, Braganhol E, et al. Inhibition of the Adenosinergic Pathway in Cancer Rejuvenates Innate and Adaptive Immunity. Int J Mol Sci 2019;20:5698.
8. Carone C, Olivani A, Dalla Valle R, et al. Immune Gene Expression Profile in Hepatocellular Carcinoma and Surrounding Tissue Predicts Time to Tumor Recurrence. Liver Cancer 2018;7:277-94.
9. Zhang FP, Huang YP, Luo WX, et al. Construction of a risk score prognosis model based on hepatocellular carcinoma microenvironment. World J Gastroenterol 2020;26:134-53.
10. Hsiao YW, Chiu LT, Chen CH, et al. Tumor-Infiltrating Leukocyte Composition and Prognostic Power in Hepatitis B- and Hepatitis C-Related Hepatocellular Carcinomas. Genes (Basel) 2019;10:630.
11. Zhao X, Chen Y, Mao Q, et al. Overexpression of YTHDF1 is associated with poor prognosis in patients with hepatocellular carcinoma. Cancer Biomark 2018;21:859-68.
12. Han M, Yang G, Lin Q, et al. Determination of Endogenous Bufalin in Serum of Patients With Hepatocellular Carcinoma Based on HPLC-MS/MS. Front Oncol 2020;9:1572.
13. Yang Z, Li J, Feng G, et al. MicroRNA-145 Modulates N6-Methyladenosine Levels by Targeting the 3'-Untranslated mRNA Region of the N6-Methyladenosine Binding YTH Domain Family 2 Protein. J Biol Chem 2017;292:3614-23.
14. Colaprico A, Silva TC, Olsen C, et al. TCGAbiolinks: an R/Bioconductor package for integrative analysis of TCGA data. Nucleic Acids Res 2016;44:e71.
15. Grossman RL. Data Lakes, Clouds, and Commons: A Review of Platforms for Analyzing and Sharing Genomic Data. Trends Genet 2019;35:223-34.
16. Wilkerson MD, Hayes DN. ConsensusClusterPlus: a class discovery tool with confidence assessments and item tracking. Bioinformatics 2010;26:1572-3.
17. Charoentong P, Finotello F, Angelova M, et al. Pan-cancer Immunogenomic Analyses Reveal Genotype-Immunophenotype Relationships and Predictors of Response to Checkpoint Blockade. Cell Rep 2017;18:248-62.
18. Zhang B, Wu Q, Li B, et al. m6A regulator-mediated methylation modification patterns and tumor microenvironment infiltration characterization in gastric cancer. Mol Cancer 2020;19:53.
19. Qin L, Min S, Shu L, et al. Genetic analysis of N6-methyladenosine modification genes in Parkinson's disease. Neurobiol Aging 2020;93:143.e9-143.e13.
20. Angell H, Galon J. From the immune contexture to the Immunoscore: the role of prognostic and predictive immune markers in cancer. Curr Opin Immunol 2013;25:261-7.
21. Tang X, Shu Z, Zhang W, et al. Clinical significance of the immune cell landscape in hepatocellular carcinoma patients with different degrees of fibrosis. Ann Transl Med 2019;7:528.
22. Zhao BS, Wang X, Beadell AV, et al. m6A-dependent maternal mRNA clearance facilitates zebrafish maternal-to-zygotic transition. Nature 2017;542:475-8.
23. Guan K, Liu X, Li J, et al. Expression Status And Prognostic Value Of M6A-associated Genes in Gastric Cancer. J Cancer 2020;11:3027-40.
24. Yuan Y, Du Y, Wang L, Liu X. The M6A methyltransferase METTL3 promotes the development and progression of prostate carcinoma via mediating MYC methylation. J Cancer 2020;11:3588-95.
25. Ling Z, Chen L, Zhao J. m6A-dependent up-regulation of DRG1 by METTL3 and ELAVL1 promotes growth, migration, and colony formation in osteosarcoma. Biosci Rep 2020;40:BSR20200282.
26. Yang X, Zhang S, He C, et al. METTL14 suppresses proliferation and metastasis of colorectal cancer by down-regulating oncogenic long non-coding RNA XIST. Mol Cancer 2020;19:46.

27. Mandelkow T, Blessin NC, Lueerss E, et al. Immune Exclusion Is Frequent in Small-Cell Carcinoma of the Bladder. Dis Markers 2019;2019:2532518.
28. Mariathasan S, Turley SJ, Nickles D, et al. TGFβ attenuates tumour response to PD-L1 blockade by contributing to exclusion of T cells. Nature 2018;554:544-8.
29. Zhao S, Ma D, Xiao Y, et al. Molecular Subtyping of Triple-Negative Breast Cancers by Immunohistochemistry: Molecular Basis and Clinical Relevance. Oncologist 2020;25:e1481-91.
30. Job S, Rapoud D, Dos Santos A, et al. Identification of four immune subtypes characterized by distinct composition and functions of tumor microenvironment in intrahepatic cholangiocarcinoma. Hepatology 2019;72:965-81.
31. Winkler R, Gillis E, Lasman L, et al. m6A modification controls the innate immune response to infection by targeting type I interferons. Nat Immunol 2019;20:173-82.
32. Han D, Liu J, Chen C, et al. Anti-tumour immunity controlled through mRNA m6A methylation and YTHDF1 in dendritic cells. Nature 2019;566:270-4.

Cite this article as: Shen S, Yan J, Zhang Y, Dong Z, Xing J, He Y. N6-methyladenosine (m6A)-mediated messenger RNA signatures and the tumor immune microenvironment can predict the prognosis of hepatocellular carcinoma. Ann Transl Med 2021;9(1):59. doi: 10.21037/atm-20-7396

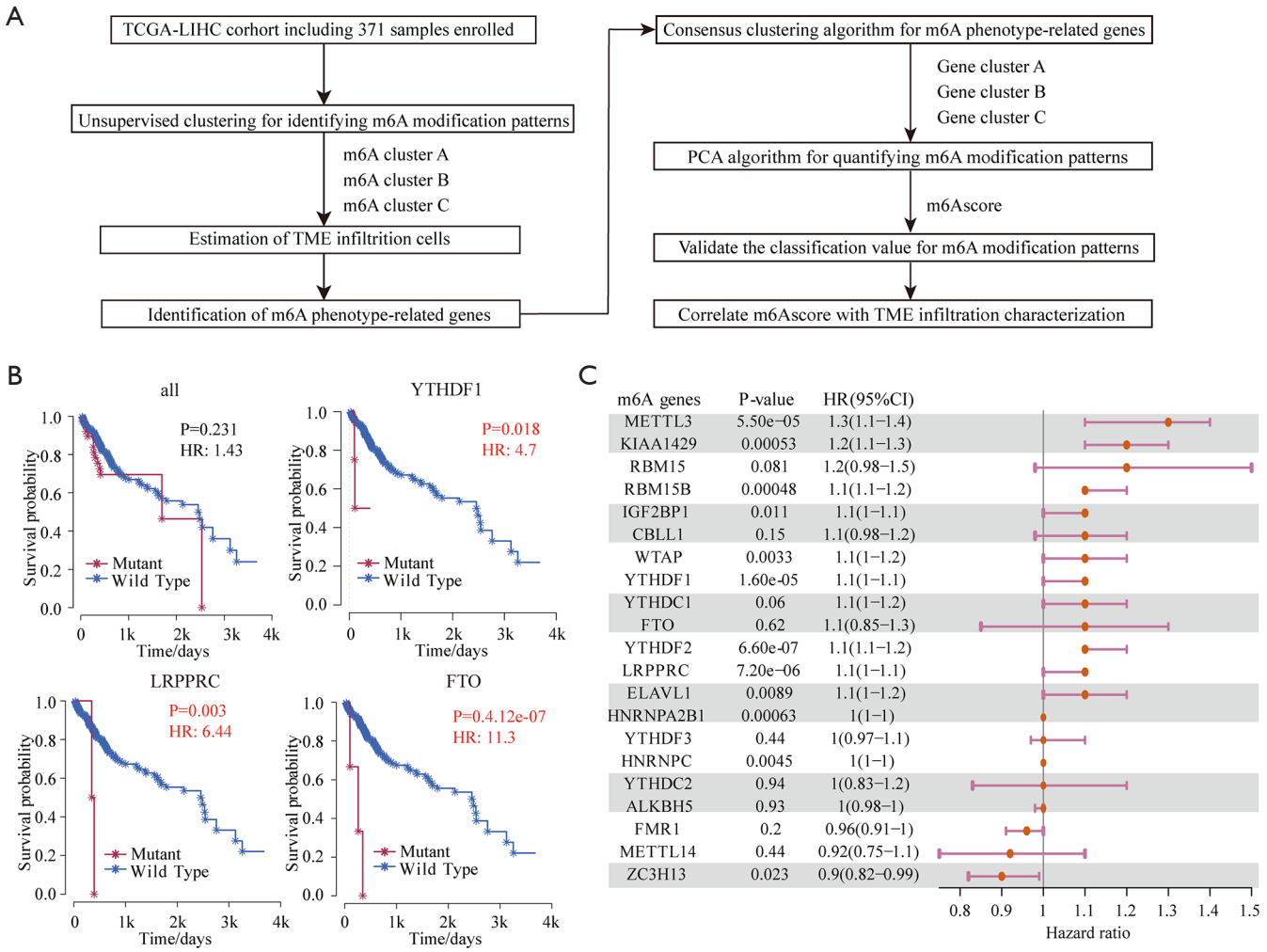

Figure S1 Work flow and survival analysis of m6A regulators. (A) Flow diagram of the analysis procedure, including data collection, preprocessing, and analysis. (B) Overall survival analysis and clinicopathological features between mutated cohort and wide type cohort of regulators. Kaplan-Meier curves of all regulators, *YTHDF1*, *LRPPRC*, and *FTO*. The red represents mutant regulators. (C) Forest plot showing different gene expression of m6A regulators and overall patient survival. m6A, N6-methyladenosine.

http://dx.doi.org/10.21037/atm-20-7396

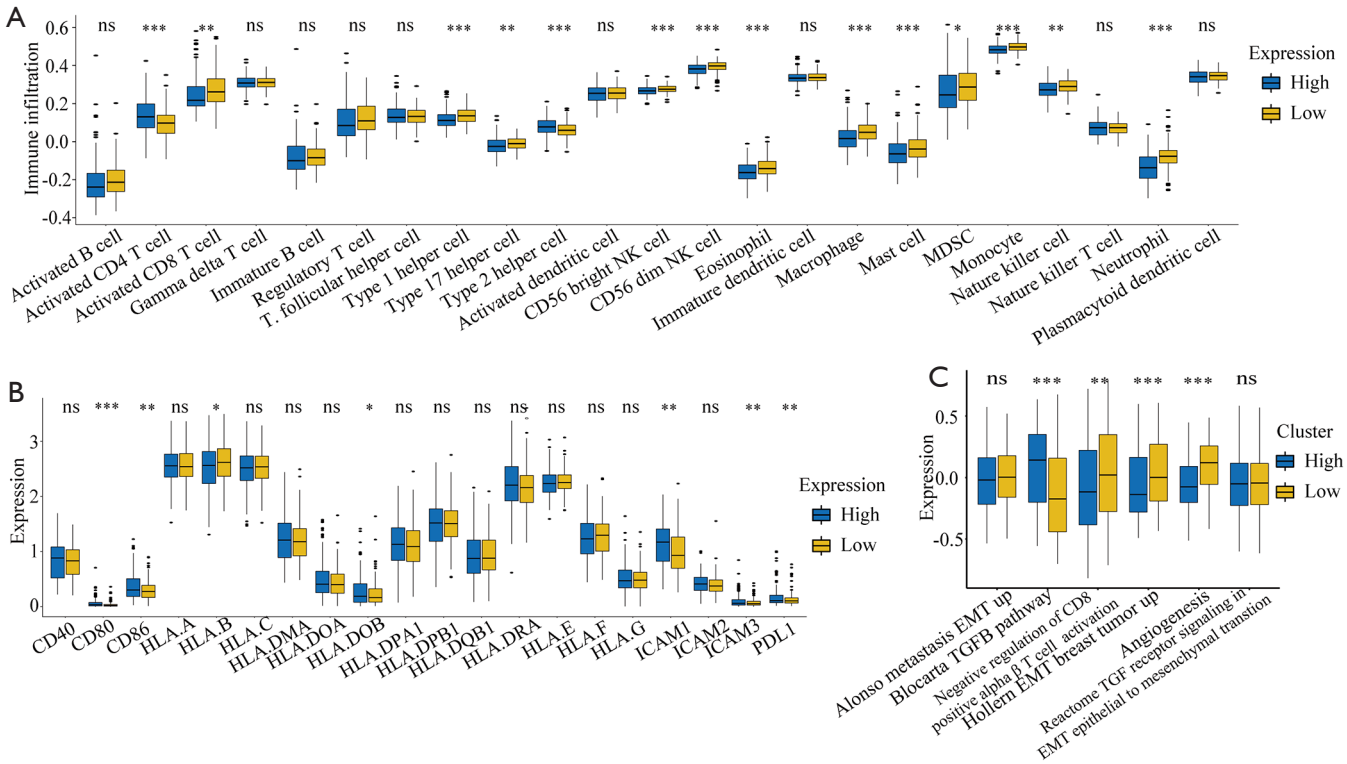

Figure S2 Different m6A regulator expression levels showed different immune cells infiltration. (A) Different *METTL3* expression levels had characteristic immune cell infiltration. (B) Different *METTL3* expression levels exhibited different immune cell infiltration. (C) Different *METTL3* expression levels showed different enriched biological pathways. m6A, N6-methyladenosine; *METTL3*, methyltransferase like 3. *P<0.05, **P<0.01, ***P<0.001.

http://dx.doi.org/10.21037/atm-20-7396

Table S1 The gene sets used in this work for marking each TME infiltration cell type

Metagene	Cell.type	Immunity
ADAM28	Activated.B.cell	Adaptive
CD180	Activated.B.cell	Adaptive
CD79B	Activated.B.cell	Adaptive
BLK	Activated.B.cell	Adaptive
CD19	Activated.B.cell	Adaptive
MS4A1	Activated.B.cell	Adaptive
TNFRSF17	Activated.B.cell	Adaptive
IGHM	Activated.B.cell	Adaptive
GNG7	Activated.B.cell	Adaptive
MICAL3	Activated.B.cell	Adaptive
SPIB	Activated.B.cell	Adaptive
HLA-DOB	Activated.B.cell	Adaptive
IGKC	Activated.B.cell	Adaptive
PNOC	Activated.B.cell	Adaptive
FCRL2	Activated.B.cell	Adaptive
BACH2	Activated.B.cell	Adaptive
CR2	Activated.B.cell	Adaptive
TCL1A	Activated.B.cell	Adaptive
AKNA	Activated.B.cell	Adaptive
ARHGAP25	Activated.B.cell	Adaptive
CCL21	Activated.B.cell	Adaptive
CD27	Activated.B.cell	Adaptive
CD38	Activated.B.cell	Adaptive
CLEC17A	Activated.B.cell	Adaptive
CLEC9A	Activated.B.cell	Adaptive
CLECL1	Activated.B.cell	Adaptive
AIM2	Activated.CD4.T.cell	Adaptive
BIRC3	Activated.CD4.T.cell	Adaptive
BRIP1	Activated.CD4.T.cell	Adaptive
CCL20	Activated.CD4.T.cell	Adaptive
CCL4	Activated.CD4.T.cell	Adaptive
CCL5	Activated.CD4.T.cell	Adaptive
CCNB1	Activated.CD4.T.cell	Adaptive
CCR7	Activated.CD4.T.cell	Adaptive
DUSP2	Activated.CD4.T.cell	Adaptive
ESCO2	Activated.CD4.T.cell	Adaptive
ETS1	Activated.CD4.T.cell	Adaptive
EXO1	Activated.CD4.T.cell	Adaptive
EXOC6	Activated.CD4.T.cell	Adaptive
IARS	Activated.CD4.T.cell	Adaptive
ITK	Activated.CD4.T.cell	Adaptive
KIF11	Activated.CD4.T.cell	Adaptive
KNTC1	Activated.CD4.T.cell	Adaptive
NUF2	Activated.CD4.T.cell	Adaptive
PRC1	Activated.CD4.T.cell	Adaptive
PSAT1	Activated.CD4.T.cell	Adaptive
RGS1	Activated.CD4.T.cell	Adaptive
RTKN2	Activated.CD4.T.cell	Adaptive
SAMSN1	Activated.CD4.T.cell	Adaptive
SELL	Activated.CD4.T.cell	Adaptive
TRAT1	Activated.CD4.T.cell	Adaptive

http://dx.doi.org/10.21037/atm-20-7396

ADRM1	Activated.CD8.T.cell	Adaptive
AHSA1	Activated.CD8.T.cell	Adaptive
C1GALT1C1	Activated.CD8.T.cell	Adaptive
CCT6B	Activated.CD8.T.cell	Adaptive
CD37	Activated.CD8.T.cell	Adaptive
CD3D	Activated.CD8.T.cell	Adaptive
CD3E	Activated.CD8.T.cell	Adaptive
CD3G	Activated.CD8.T.cell	Adaptive
CD69	Activated.CD8.T.cell	Adaptive
CD8A	Activated.CD8.T.cell	Adaptive
CETN3	Activated.CD8.T.cell	Adaptive
CSE1L	Activated.CD8.T.cell	Adaptive
GEMIN6	Activated.CD8.T.cell	Adaptive
GNLY	Activated.CD8.T.cell	Adaptive
GPT2	Activated.CD8.T.cell	Adaptive
GZMA	Activated.CD8.T.cell	Adaptive
GZMH	Activated.CD8.T.cell	Adaptive
GZMK	Activated.CD8.T.cell	Adaptive
IL2RB	Activated.CD8.T.cell	Adaptive
LCK	Activated.CD8.T.cell	Adaptive
MPZL1	Activated.CD8.T.cell	Adaptive
NKG7	Activated.CD8.T.cell	Adaptive
PIK3IP1	Activated.CD8.T.cell	Adaptive
PTRH2	Activated.CD8.T.cell	Adaptive
TIMM13	Activated.CD8.T.cell	Adaptive
ZAP70	Activated.CD8.T.cell	Adaptive
ACP5	Gamma.delta.T.cell	Adaptive
AQP9	Gamma.delta.T.cell	Adaptive
BTN3A2	Gamma.delta.T.cell	Adaptive
C1orf54	Gamma.delta.T.cell	Adaptive
CARD8	Gamma.delta.T.cell	Adaptive
CCL18	Gamma.delta.T.cell	Adaptive
CD209	Gamma.delta.T.cell	Adaptive
CD33	Gamma.delta.T.cell	Adaptive
CD36	Gamma.delta.T.cell	Adaptive
CDK5	Gamma.delta.T.cell	Adaptive
IL10RB	Gamma.delta.T.cell	Adaptive
KLRF1	Gamma.delta.T.cell	Adaptive
LGALS1	Gamma.delta.T.cell	Adaptive
MAPK7	Gamma.delta.T.cell	Adaptive
KLHL7	Gamma.delta.T.cell	Adaptive
KRT80	Gamma.delta.T.cell	Adaptive
LAMC1	Gamma.delta.T.cell	Adaptive
LCORL	Gamma.delta.T.cell	Adaptive
LMNB1	Gamma.delta.T.cell	Adaptive
MEIS3P1	Gamma.delta.T.cell	Adaptive
MPL	Gamma.delta.T.cell	Adaptive
FABP1	Gamma.delta.T.cell	Adaptive
FABP5	Gamma.delta.T.cell	Adaptive
FADD	Gamma.delta.T.cell	Adaptive
MFAP3L	Gamma.delta.T.cell	Adaptive
MINPP1	Gamma.delta.T.cell	Adaptive
RPS24	Gamma.delta.T.cell	Adaptive
RPS7	Gamma.delta.T.cell	Adaptive

http://dx.doi.org/10.21037/atm-20-7396

RPS9	Gamma.delta.T.cell	Adaptive
DBNL	Gamma.delta.T.cell	Adaptive
CCL13	Gamma.delta.T.cell	Adaptive
CD22	Immature..B.cell	Adaptive
CYBB	Immature..B.cell	Adaptive
FAM129C	Immature..B.cell	Adaptive
FCRL1	Immature..B.cell	Adaptive
FCRL3	Immature..B.cell	Adaptive
FCRL5	Immature..B.cell	Adaptive
FCRLA	Immature..B.cell	Adaptive
HDAC9	Immature..B.cell	Adaptive
HLA-DQA1	Immature..B.cell	Adaptive
HVCN1	Immature..B.cell	Adaptive
KIAA0226	Immature..B.cell	Adaptive
NCF1	Immature..B.cell	Adaptive
NCF1B	Immature..B.cell	Adaptive
P2RY10	Immature..B.cell	Adaptive
SP100	Immature..B.cell	Adaptive
TXNIP	Immature..B.cell	Adaptive
STAP1	Immature..B.cell	Adaptive
TAGAP	Immature..B.cell	Adaptive
ZCCHC2	Immature..B.cell	Adaptive
CCL3L1	Regulatory.T.cell	Adaptive
CD72	Regulatory.T.cell	Adaptive
CLEC5A	Regulatory.T.cell	Adaptive
FOXP3	Regulatory.T.cell	Adaptive
ITGA4	Regulatory.T.cell	Adaptive
L1CAM	Regulatory.T.cell	Adaptive
LIPA	Regulatory.T.cell	Adaptive
LRP1	Regulatory.T.cell	Adaptive
LRRC42	Regulatory.T.cell	Adaptive
MARCO	Regulatory.T.cell	Adaptive
MMP12	Regulatory.T.cell	Adaptive
MNDA	Regulatory.T.cell	Adaptive
MRC1	Regulatory.T.cell	Adaptive
MS4A6A	Regulatory.T.cell	Adaptive
PELO	Regulatory.T.cell	Adaptive
PLEK	Regulatory.T.cell	Adaptive
PRSS23	Regulatory.T.cell	Adaptive
PTGIR	Regulatory.T.cell	Adaptive
ST8SIA4	Regulatory.T.cell	Adaptive
STAB1	Regulatory.T.cell	Adaptive
B3GAT1	T.follicular.helper.cell	Adaptive
CDK5R1	T.follicular.helper.cell	Adaptive
PDCD1	T.follicular.helper.cell	Adaptive
BCL6	T.follicular.helper.cell	Adaptive
CD200	T.follicular.helper.cell	Adaptive
CD83	T.follicular.helper.cell	Adaptive
CD84	T.follicular.helper.cell	Adaptive
FGF2	T.follicular.helper.cell	Adaptive
GPR18	T.follicular.helper.cell	Adaptive
CEBPA	T.follicular.helper.cell	Adaptive
CECR1	T.follicular.helper.cell	Adaptive
CLEC10A	T.follicular.helper.cell	Adaptive

http://dx.doi.org/10.21037/atm-20-7396

CLEC4A	T.follicular.helper.cell	Adaptive
CSF1R	T.follicular.helper.cell	Adaptive
CTSS	T.follicular.helper.cell	Adaptive
DMN	T.follicular.helper.cell	Adaptive
DPP4	T.follicular.helper.cell	Adaptive
LRRC32	T.follicular.helper.cell	Adaptive
MC5R	T.follicular.helper.cell	Adaptive
MICA	T.follicular.helper.cell	Adaptive
NCAM1	T.follicular.helper.cell	Adaptive
NCR2	T.follicular.helper.cell	Adaptive
NRP1	T.follicular.helper.cell	Adaptive
PDCD1LG2	T.follicular.helper.cell	Adaptive
PDCD6	T.follicular.helper.cell	Adaptive
PRDX1	T.follicular.helper.cell	Adaptive
RAE1	T.follicular.helper.cell	Adaptive
RAET1E	T.follicular.helper.cell	Adaptive
SIGLEC7	T.follicular.helper.cell	Adaptive
SIGLEC9	T.follicular.helper.cell	Adaptive
TYRO3	T.follicular.helper.cell	Adaptive
CHST12	T.follicular.helper.cell	Adaptive
CLIC3	T.follicular.helper.cell	Adaptive
IVNS1ABP	T.follicular.helper.cell	Adaptive
KIR2DL2	T.follicular.helper.cell	Adaptive
LGMN	T.follicular.helper.cell	Adaptive
CD70	Type.1.T.helper.cell	Adaptive
TBX21	Type.1.T.helper.cell	Adaptive
ADAM8	Type.1.T.helper.cell	Adaptive
AHCYL2	Type.1.T.helper.cell	Adaptive
ALCAM	Type.1.T.helper.cell	Adaptive
B3GALNT1	Type.1.T.helper.cell	Adaptive
BBS12	Type.1.T.helper.cell	Adaptive
BST1	Type.1.T.helper.cell	Adaptive
CD151	Type.1.T.helper.cell	Adaptive
CD47	Type.1.T.helper.cell	Adaptive
CD48	Type.1.T.helper.cell	Adaptive
CD52	Type.1.T.helper.cell	Adaptive
CD53	Type.1.T.helper.cell	Adaptive
CD59	Type.1.T.helper.cell	Adaptive
CD6	Type.1.T.helper.cell	Adaptive
CD68	Type.1.T.helper.cell	Adaptive
CD7	Type.1.T.helper.cell	Adaptive
CD96	Type.1.T.helper.cell	Adaptive
CFHR3	Type.1.T.helper.cell	Adaptive
CHRM3	Type.1.T.helper.cell	Adaptive
CLEC7A	Type.1.T.helper.cell	Adaptive
COL23A1	Type.1.T.helper.cell	Adaptive
COL4A4	Type.1.T.helper.cell	Adaptive
COL5A3	Type.1.T.helper.cell	Adaptive
DAB1	Type.1.T.helper.cell	Adaptive
DLEU7	Type.1.T.helper.cell	Adaptive
DOC2B	Type.1.T.helper.cell	Adaptive
EMP1	Type.1.T.helper.cell	Adaptive
F12	Type.1.T.helper.cell	Adaptive
FURIN	Type.1.T.helper.cell	Adaptive

http://dx.doi.org/10.21037/atm-20-7396

GAB3	Type.1.T.helper.cell	Adaptive
GATM	Type.1.T.helper.cell	Adaptive
GFPT2	Type.1.T.helper.cell	Adaptive
GPR25	Type.1.T.helper.cell	Adaptive
GREM2	Type.1.T.helper.cell	Adaptive
HAVCR1	Type.1.T.helper.cell	Adaptive
HSD11B1	Type.1.T.helper.cell	Adaptive
HUNK	Type.1.T.helper.cell	Adaptive
IGF2	Type.1.T.helper.cell	Adaptive
RCSD1	Type.1.T.helper.cell	Adaptive
RYR1	Type.1.T.helper.cell	Adaptive
SAV1	Type.1.T.helper.cell	Adaptive
SELE	Type.1.T.helper.cell	Adaptive
SELP	Type.1.T.helper.cell	Adaptive
SH3KBP1	Type.1.T.helper.cell	Adaptive
SIT1	Type.1.T.helper.cell	Adaptive
SLC35B3	Type.1.T.helper.cell	Adaptive
SIGLEC10	Type.1.T.helper.cell	Adaptive
SKAP1	Type.1.T.helper.cell	Adaptive
THUMPD2	Type.1.T.helper.cell	Adaptive
TIGIT	Type.1.T.helper.cell	Adaptive
ZEB2	Type.1.T.helper.cell	Adaptive
ENC1	Type.1.T.helper.cell	Adaptive
FAM134B	Type.1.T.helper.cell	Adaptive
FBXO30	Type.1.T.helper.cell	Adaptive
FCGR2C	Type.1.T.helper.cell	Adaptive
STAC	Type.1.T.helper.cell	Adaptive
LTC4S	Type.1.T.helper.cell	Adaptive
MAN1B1	Type.1.T.helper.cell	Adaptive
MDH1	Type.1.T.helper.cell	Adaptive
MMD	Type.1.T.helper.cell	Adaptive
RGS16	Type.1.T.helper.cell	Adaptive
IL12A	Type.1.T.helper.cell	Adaptive
P2RX5	Type.1.T.helper.cell	Adaptive
CD97	Type.1.T.helper.cell	Adaptive
ITGB4	Type.1.T.helper.cell	Adaptive
ICAM3	Type.1.T.helper.cell	Adaptive
METRNL	Type.1.T.helper.cell	Adaptive
TNFRSF1A	Type.1.T.helper.cell	Adaptive
IRF1	Type.1.T.helper.cell	Adaptive
HTR2B	Type.1.T.helper.cell	Adaptive
CALD1	Type.1.T.helper.cell	Adaptive
MOCOS	Type.1.T.helper.cell	Adaptive
TRAF3IP2	Type.1.T.helper.cell	Adaptive
TLR8	Type.1.T.helper.cell	Adaptive
TRAF1	Type.1.T.helper.cell	Adaptive
DUSP14	Type.1.T.helper.cell	Adaptive
IL17A	Type.17.T.helper.cell	Adaptive
IL17RA	Type.17.T.helper.cell	Adaptive
C2CD4A	Type.17.T.helper.cell	Adaptive
C2CD4B	Type.17.T.helper.cell	Adaptive
CA2	Type.17.T.helper.cell	Adaptive
CCDC65	Type.17.T.helper.cell	Adaptive
CEACAM3	Type.17.T.helper.cell	Adaptive

http://dx.doi.org/10.21037/atm-20-7396

IL17C	Type.17.T.helper.cell	Adaptive
IL17F	Type.17.T.helper.cell	Adaptive
IL17RC	Type.17.T.helper.cell	Adaptive
IL17RE	Type.17.T.helper.cell	Adaptive
IL23A	Type.17.T.helper.cell	Adaptive
ILDR1	Type.17.T.helper.cell	Adaptive
LONRF3	Type.17.T.helper.cell	Adaptive
SH2D6	Type.17.T.helper.cell	Adaptive
TNIP2	Type.17.T.helper.cell	Adaptive
ABCA1	Type.17.T.helper.cell	Adaptive
ABCB1	Type.17.T.helper.cell	Adaptive
ADAMTS12	Type.17.T.helper.cell	Adaptive
ANK1	Type.17.T.helper.cell	Adaptive
ANKRD22	Type.17.T.helper.cell	Adaptive
B3GALT2	Type.17.T.helper.cell	Adaptive
CAMTA1	Type.17.T.helper.cell	Adaptive
CCR9	Type.17.T.helper.cell	Adaptive
CD40	Type.17.T.helper.cell	Adaptive
GPR44	Type.17.T.helper.cell	Adaptive
IFT80	Type.17.T.helper.cell	Adaptive
ASB2	Type.2.T.helper.cell	Adaptive
CSRP2	Type.2.T.helper.cell	Adaptive
DAPK1	Type.2.T.helper.cell	Adaptive
DLC1	Type.2.T.helper.cell	Adaptive
DNAJC12	Type.2.T.helper.cell	Adaptive
DUSP6	Type.2.T.helper.cell	Adaptive
GNAI1	Type.2.T.helper.cell	Adaptive
LAMP3	Type.2.T.helper.cell	Adaptive
NRP2	Type.2.T.helper.cell	Adaptive
OSBPL1A	Type.2.T.helper.cell	Adaptive
PDE4B	Type.2.T.helper.cell	Adaptive
PHLDA1	Type.2.T.helper.cell	Adaptive
PLA2G4A	Type.2.T.helper.cell	Adaptive
RAB27B	Type.2.T.helper.cell	Adaptive
RBMS3	Type.2.T.helper.cell	Adaptive
RNF125	Type.2.T.helper.cell	Adaptive
TMPRSS3	Type.2.T.helper.cell	Adaptive
GATA3	Type.2.T.helper.cell	Adaptive
BIRC5	Type.2.T.helper.cell	Adaptive
CDC25C	Type.2.T.helper.cell	Adaptive
CDC7	Type.2.T.helper.cell	Adaptive
CENPF	Type.2.T.helper.cell	Adaptive
CXCR6	Type.2.T.helper.cell	Adaptive
DHFR	Type.2.T.helper.cell	Adaptive
EVI5	Type.2.T.helper.cell	Adaptive
GSTA4	Type.2.T.helper.cell	Adaptive
HELLS	Type.2.T.helper.cell	Adaptive
IL26	Type.2.T.helper.cell	Adaptive
LAIR2	Type.2.T.helper.cell	Adaptive
ABCD1	Activated.dendritic.cell	Innate
C1QC	Activated.dendritic.cell	Innate
CAPG	Activated.dendritic.cell	Innate
CCL3L3	Activated.dendritic.cell	Innate
CD207	Activated.dendritic.cell	Innate

http://dx.doi.org/10.21037/atm-20-7396

CD302	Activated.dendritic.cell	Innate
ATP5B	Activated.dendritic.cell	Innate
ATP5L	Activated.dendritic.cell	Innate
ATP6V1A	Activated.dendritic.cell	Innate
BCL2L1	Activated.dendritic.cell	Innate
C1QB	Activated.dendritic.cell	Innate
SNURF	Activated.dendritic.cell	Innate
SPCS3	Activated.dendritic.cell	Innate
CCNA1	Activated.dendritic.cell	Innate
CEACAM8	Activated.dendritic.cell	Innate
NOS2	Activated.dendritic.cell	Innate
SRA1	Activated.dendritic.cell	Innate
TNFRSF6B	Activated.dendritic.cell	Innate
TREM1	Activated.dendritic.cell	Innate
TREML1	Activated.dendritic.cell	Innate
RHOA	Activated.dendritic.cell	Innate
SLC25A37	Activated.dendritic.cell	Innate
TNFSF14	Activated.dendritic.cell	Innate
TREML4	Activated.dendritic.cell	Innate
VNN2	Activated.dendritic.cell	Innate
XPO6	Activated.dendritic.cell	Innate
CLEC4C	Activated.dendritic.cell	Innate
TNFAIP2	Activated.dendritic.cell	Innate
UBD	Activated.dendritic.cell	Innate
ACTR3	Activated.dendritic.cell	Innate
RAB1A	Activated.dendritic.cell	Innate
SLA	Activated.dendritic.cell	Innate
HLA-DQA2	Activated.dendritic.cell	Innate
SIGLEC5	Activated.dendritic.cell	Innate
SLAMF9	Activated.dendritic.cell	Innate
ABAT	CD56bright.natural.killer.ce	Innate
C11orf75	CD56bright.natural.killer.ce	Innate
C5orf15	CD56bright.natural.killer.ce	Innate
CDHR1	CD56bright.natural.killer.ce	Innate
DCAF12	CD56bright.natural.killer.ce	Innate
DYNLL1	CD56bright.natural.killer.ce	Innate
GPR137B	CD56bright.natural.killer.ce	Innate
HCP5	CD56bright.natural.killer.ce	Innate
HDGFRP2	CD56bright.natural.killer.ce	Innate
KRT86	CD56bright.natural.killer.ce	Innate
MLST8	CD56bright.natural.killer.ce	Innate
ELMOD3	CD56bright.natural.killer.ce	Innate
ENTPD5	CD56bright.natural.killer.ce	Innate
FAM119A	CD56bright.natural.killer.ce	Innate
FAM179A	CD56bright.natural.killer.ce	Innate
CLIC2	CD56bright.natural.killer.ce	Innate
COX7A2L	CD56bright.natural.killer.ce	Innate
CREB3L4	CD56bright.natural.killer.ce	Innate
CSF1	CD56bright.natural.killer.ce	Innate
CSNK2A2	CD56bright.natural.killer.ce	Innate
CSTA	CD56bright.natural.killer.ce	Innate
CSTB	CD56bright.natural.killer.ce	Innate
CTPS	CD56bright.natural.killer.ce	Innate
CTSD	CD56bright.natural.killer.ce	Innate

http://dx.doi.org/10.21037/atm-20-7396

FST	CD56bright.natural.killer.ce	Innate
GATA2	CD56bright.natural.killer.ce	Innate
GMPR	CD56bright.natural.killer.ce	Innate
HDC	CD56bright.natural.killer.ce	Innate
HEY1	CD56bright.natural.killer.ce	Innate
HOXA1	CD56bright.natural.killer.ce	Innate
HS2ST1	CD56bright.natural.killer.ce	Innate
HS3ST1	CD56bright.natural.killer.ce	Innate
BCL11B	CD56bright.natural.killer.ce	Innate
CDH3	CD56bright.natural.killer.ce	Innate
MYL6B	CD56bright.natural.killer.ce	Innate
NAA16	CD56bright.natural.killer.ce	Innate
ClQA	CD56bright.natural.killer.ce	Innate
ClQB	CD56bright.natural.killer.ce	Innate
CYP27B1	CD56bright.natural.killer.ce	Innate
EIF3M	CD56bright.natural.killer.ce	Innate
CYP27A1	CD56dim.natural.killer.cell	Innate
DDX55	CD56dim.natural.killer.cell	Innate
DYRK2	CD56dim.natural.killer.cell	Innate
RPL37A	CD56dim.natural.killer.cell	Innate
NOTCH3	CD56dim.natural.killer.cell	Innate
AKR7A3	CD56dim.natural.killer.cell	Innate
GPRC5C	CD56dim.natural.killer.cell	Innate
GRIN1	CD56dim.natural.killer.cell	Innate
HLA-E	CD56dim.natural.killer.cell	Innate
PORCN	CD56dim.natural.killer.cell	Innate
PSMC4	CD56dim.natural.killer.cell	Innate
UPP1	CD56dim.natural.killer.cell	Innate
IL21R	CD56dim.natural.killer.cell	Innate
KIR2DS1	CD56dim.natural.killer.cell	Innate
KIR2DS2	CD56dim.natural.killer.cell	Innate
KIR2DS5	CD56dim.natural.killer.cell	Innate
GIPR	Eosinophil	Innate
KRT18P50	Eosinophil	Innate
LRMP	Eosinophil	Innate
FOSB	Eosinophil	Innate
RRP12	Eosinophil	Innate
GPR183	Eosinophil	Innate
NR4A3	Eosinophil	Innate
ST3GAL6	Eosinophil	Innate
DEPDC5	Eosinophil	Innate
PDE6C	Eosinophil	Innate
PKD2L2	Eosinophil	Innate
GPR65	Eosinophil	Innate
IL5RA	Eosinophil	Innate
P2RY14	Eosinophil	Innate
DACH1	Eosinophil	Innate
DAPK2	Eosinophil	Innate
EMR3	Eosinophil	Innate
ACADM	Immature.dendritic.cell	Innate
AHCYL1	Immature.dendritic.cell	Innate
ALDH1A2	Immature.dendritic.cell	Innate
ALDH3A2	Immature.dendritic.cell	Innate
ALDH9A1	Immature.dendritic.cell	Innate

http://dx.doi.org/10.21037/atm-20-7396

ALOX15	Immature.dendritic.cell	Innate
AMT	Immature.dendritic.cell	Innate
ARL1	Immature.dendritic.cell	Innate
ATIC	Immature.dendritic.cell	Innate
ATP5A1	Immature.dendritic.cell	Innate
CAPZA1	Immature.dendritic.cell	Innate
LILRA5	Immature.dendritic.cell	Innate
RDX	Immature.dendritic.cell	Innate
RRAGD	Immature.dendritic.cell	Innate
TACSTD2	Immature.dendritic.cell	Innate
INPP5F	Immature.dendritic.cell	Innate
RAB38	Immature.dendritic.cell	Innate
PLAU	Immature.dendritic.cell	Innate
CSF3R	Immature.dendritic.cell	Innate
SLC18A2	Immature.dendritic.cell	Innate
AMPD2	Immature.dendritic.cell	Innate
CLTB	Immature.dendritic.cell	Innate
C1orf162	Immature.dendritic.cell	Innate
AIF1	Macrophage	Innate
CCL1	Macrophage	Innate
CCL14	Macrophage	Innate
CCL23	Macrophage	Innate
CCL26	Macrophage	Innate
CD300LB	Macrophage	Innate
CNR1	Macrophage	Innate
CNR2	Macrophage	Innate
EIF1	Macrophage	Innate
EIF4A1	Macrophage	Innate
FPR1	Macrophage	Innate
FPR2	Macrophage	Innate
FRAT2	Macrophage	Innate
GPR27	Macrophage	Innate
GPR77	Macrophage	Innate
RNASE2	Macrophage	Innate
MS4A2	Macrophage	Innate
BASP1	Macrophage	Innate
IGSF6	Macrophage	Innate
HK3	Macrophage	Innate
VNN1	Macrophage	Innate
FES	Macrophage	Innate
NPL	Macrophage	Innate
FZD2	Macrophage	Innate
FAM198B	Macrophage	Innate
HNMT	Macrophage	Innate
SLC15A3	Macrophage	Innate
CD4	Macrophage	Innate
TXNDC3	Macrophage	Innate
FRMD4A	Macrophage	Innate
CRYBB1	Macrophage	Innate
HRH1	Macrophage	Innate
WNT5B	Macrophage	Innate
ADAMTS3	Mast.cell	Innate
CPA3	Mast.cell	Innate
CMA1	Mast.cell	Innate

http://dx.doi.org/10.21037/atm-20-7396

CTSG	Mast.cell	Innate
ARHGAP15	Mast.cell	Innate
CPM	Mast.cell	Innate
FCN1	Mast.cell	Innate
FTL	Mast.cell	Innate
HSPA6	Mast.cell	Innate
ITGA9	Mast.cell	Innate
RNASE3	Mast.cell	Innate
S100A4	Mast.cell	Innate
SIGLEC8	Mast.cell	Innate
SLC6A4	Mast.cell	Innate
PTGS2	Mast.cell	Innate
EGR3	Mast.cell	Innate
PILRA	Mast.cell	Innate
CCR2	MDSC	Innate
CD14	MDSC	Innate
CD2	MDSC	Innate
CD86	MDSC	Innate
CXCR4	MDSC	Innate
FCGR2A	MDSC	Innate
FCGR2B	MDSC	Innate
FCGR3A	MDSC	Innate
FERMT3	MDSC	Innate
GPSM3	MDSC	Innate
IL18BP	MDSC	Innate
IL4R	MDSC	Innate
ITGAL	MDSC	Innate
ITGAM	MDSC	Innate
PARVG	MDSC	Innate
PSAP	MDSC	Innate
PTGER2	MDSC	Innate
PTGES2	MDSC	Innate
S100A8	MDSC	Innate
S100A9	MDSC	Innate
ASGR2	Monocyte	Innate
CFP	Monocyte	Innate
ASGR1	Monocyte	Innate
CD1D	Monocyte	Innate
UPK3A	Monocyte	Innate
ACTG1	Monocyte	Innate
ANXA5	Monocyte	Innate
ATP6V1B2	Monocyte	Innate
CFL1	Monocyte	Innate
DAZAP2	Monocyte	Innate
CTBS	Monocyte	Innate
EMR4P	Monocyte	Innate
HIVEP2	Monocyte	Innate
MARCKSL1	Monocyte	Innate
MBP	Monocyte	Innate
MMP15	Monocyte	Innate
PNPLA6	Monocyte	Innate
TMBIM6	Monocyte	Innate
PQBP1	Monocyte	Innate
TEX264	Monocyte	Innate

http://dx.doi.org/10.21037/atm-20-7396

IKZF1	Monocyte	Innate
AKT3	Natural.killer.cell	Innate
AXL	Natural.killer.cell	Innate
BST2	Natural.killer.cell	Innate
CDH2	Natural.killer.cell	Innate
CRTAM	Natural.killer.cell	Innate
CSF2RA	Natural.killer.cell	Innate
CTSZ	Natural.killer.cell	Innate
CXCL1	Natural.killer.cell	Innate
CYTH1	Natural.killer.cell	Innate
DAXX	Natural.killer.cell	Innate
DGKH	Natural.killer.cell	Innate
DLL4	Natural.killer.cell	Innate
DPYD	Natural.killer.cell	Innate
ERBB3	Natural.killer.cell	Innate
F11R	Natural.killer.cell	Innate
FAM27A	Natural.killer.cell	Innate
FAM49A	Natural.killer.cell	Innate
FASLG	Natural.killer.cell	Innate
FCGR1A	Natural.killer.cell	Innate
FN1	Natural.killer.cell	Innate
FSTL1	Natural.killer.cell	Innate
FUCA1	Natural.killer.cell	Innate
GBP3	Natural.killer.cell	Innate
GLS2	Natural.killer.cell	Innate
GRB2	Natural.killer.cell	Innate
LST1	Natural.killer.cell	Innate
BCL2	Natural.killer.cell	Innate
CDC5L	Natural.killer.cell	Innate
FGF18	Natural.killer.cell	Innate
FUT5	Natural.killer.cell	Innate
FZR1	Natural.killer.cell	Innate
GAGE2	Natural.killer.cell	Innate
IGFBP5	Natural.killer.cell	Innate
KANK2	Natural.killer.cell	Innate
LDB3	Natural.killer.cell	Innate
BTN2A2	Natural.killer.T.cell	Innate
CD101	Natural.killer.T.cell	Innate
CD109	Natural.killer.T.cell	Innate
CNPY3	Natural.killer.T.cell	Innate
CNPY4	Natural.killer.T.cell	Innate
CREB1	Natural.killer.T.cell	Innate
CRTC2	Natural.killer.T.cell	Innate
CRTC3	Natural.killer.T.cell	Innate
CSF2	Natural.killer.T.cell	Innate
KLRC1	Natural.killer.T.cell	Innate
FUT4	Natural.killer.T.cell	Innate
ICAM2	Natural.killer.T.cell	Innate
IL32	Natural.killer.T.cell	Innate
LAMP2	Natural.killer.T.cell	Innate
LILRB5	Natural.killer.T.cell	Innate
KLRG1	Natural.killer.T.cell	Innate
HSPA4	Natural.killer.T.cell	Innate
HSPB6	Natural.killer.T.cell	Innate

http://dx.doi.org/10.21037/atm-20-7396

ISM2	Natural.killer.T.cell	Innate
ITIH2	Natural.killer.T.cell	Innate
KDM4C	Natural.killer.T.cell	Innate
KIR2DS4	Natural.killer.T.cell	Innate
KIRREL3	Natural.killer.T.cell	Innate
SDCBP	Natural.killer.T.cell	Innate
NFATC2IP	Natural.killer.T.cell	Innate
MICB	Natural.killer.T.cell	Innate
KIR2DL1	Natural.killer.T.cell	Innate
KIR2DL3	Natural.killer.T.cell	Innate
KIR3DL1	Natural.killer.T.cell	Innate
KIR3DL2	Natural.killer.T.cell	Innate
NCR1	Natural.killer.T.cell	Innate
FOSL1	Natural.killer.T.cell	Innate
TSLP	Natural.killer.T.cell	Innate
SLC7A7	Natural.killer.T.cell	Innate
SPP1	Natural.killer.T.cell	Innate
TREM2	Natural.killer.T.cell	Innate
UBASH3A	Natural.killer.T.cell	Innate
YBX2	Natural.killer.T.cell	Innate
CCDC88A	Natural.killer.T.cell	Innate
CLEC1A	Natural.killer.T.cell	Innate
THBD	Natural.killer.T.cell	Innate
PDPN	Natural.killer.T.cell	Innate
VCAM1	Natural.killer.T.cell	Innate
EMR1	Natural.killer.T.cell	Innate
CREB5	Neutrophil	Innate
CDA	Neutrophil	Innate
CHST15	Neutrophil	Innate
S100A12	Neutrophil	Innate
APOBEC3A	Neutrophil	Innate
CASP5	Neutrophil	Innate
MMP25	Neutrophil	Innate
HAL	Neutrophil	Innate
C1orf183	Neutrophil	Innate
FFAR2	Neutrophil	Innate
MAK	Neutrophil	Innate
CXCR1	Neutrophil	Innate
STEAP4	Neutrophil	Innate
MGAM	Neutrophil	Innate
BTNL8	Neutrophil	Innate
CXCR2	Neutrophil	Innate
TNFRSF10C	Neutrophil	Innate
VNN3	Neutrophil	Innate
CBX6	Plasmacytoid.dendritic.cell	Innate
DAB2	Plasmacytoid.dendritic.cell	Innate
DDX17	Plasmacytoid.dendritic.cell	Innate
HIGD1A	Plasmacytoid.dendritic.cell	Innate
IDH3A	Plasmacytoid.dendritic.cell	Innate
IL3RA	Plasmacytoid.dendritic.cell	Innate
MAGED1	Plasmacytoid.dendritic.cell	Innate
NUCB2	Plasmacytoid.dendritic.cell	Innate
OFD1	Plasmacytoid.dendritic.cell	Innate
OGT	Plasmacytoid.dendritic.cell	Innate

http://dx.doi.org/10.21037/atm-20-7396

PDIA4	Plasmacytoid.dendritic.cell	Innate
SERTAD2	Plasmacytoid.dendritic.cell	Innate
SIRPA	Plasmacytoid.dendritic.cell	Innate
TMED2	Plasmacytoid.dendritic.cell	Innate
ENG	Plasmacytoid.dendritic.cell	Innate
FCAR	Plasmacytoid.dendritic.cell	Innate
IGF1	Plasmacytoid.dendritic.cell	Innate
ITGA2B	Plasmacytoid.dendritic.cell	Innate
GABARAP	Plasmacytoid.dendritic.cell	Innate
GPX1	Plasmacytoid.dendritic.cell	Innate
KRT23	Plasmacytoid.dendritic.cell	Innate
PROK2	Plasmacytoid.dendritic.cell	Innate
RALB	Plasmacytoid.dendritic.cell	Innate
RETNLB	Plasmacytoid.dendritic.cell	Innate
RNF141	Plasmacytoid.dendritic.cell	Innate
SEC14L1	Plasmacytoid.dendritic.cell	Innate
SEPX1	Plasmacytoid.dendritic.cell	Innate
EMP3	Plasmacytoid.dendritic.cell	Innate
CD300LF	Plasmacytoid.dendritic.cell	Innate
ABTB1	Plasmacytoid.dendritic.cell	Innate
KLHL21	Plasmacytoid.dendritic.cell	Innate
PHRF1	Plasmacytoid.dendritic.cell	Innate

http://dx.doi.org/10.21037/atm-20-7396